Journal of Engineering and Development, Vol. 18, No.5, September 2014, ISSN 1813- 7822

Modeling of Viscoelastic Contact and Grasping Stability of Hemicylindrical Fingertips for Robotic and Prosthetic Hands

Lecturer. Dr. Sadeq Hussein Bakhy
Department of Machines and Equipment Engineering, University of Technology
sadeqbakhy@yahoo.com

Abstract :

Viscoelastic contact problems are one of the most important problems in mechanical and robot engineering. These problems become more tedious when one of the contacting bodies carries a viscoelastic and soft material. In this study, the mathematical model of contact interface and limit surface for viscoelastic contact which can be applied to robotic and prosthetic hemicylindrical fingertips has been proposed. The new achievement of this research comprises the integration of the time-dependent nature of viscoelastic contact into the modeling of grasping and manipulation. Specifically, two conjugation equations to get together the two significant parameters of contact modeling (the half width of rectangular contact area and the profile of pressure distribution across the contact interface) have been suggested. Additionally, two cases viable to prosthetic and robotic hands for grasping have been studied: constant rectangular contact area and constant normal contact force. The results show that the control of the grasp contact forces (case 2) when employing viscoelastic contacts is most advantageous, because it promotes the stability of grasping through the enlargement domain of limit surface as time terminates. Finally, the viscoelastic limit surface results proved that the new mathematical model is more effective (18-22%) than previous models.

Keywords: Viscoelastic contact, hemicylindrical fingertip, soft material, nonlinear elastic.

نمذجة التماس اللزج المرن و استقرارية المسكة لإطراف الأصابع النصف اسطوانية للأيدي الاصطناعية و الروبوتية

م.د. صادق حسين باخي
قسم هندسة المكائن والمعدات – الجامعة التكنولوجية

الخلاصة :

مسائل التماس اللزج المرن واحدة من المشاكل الهندسية الأكثر أهمية، وعندما يكون احد الاجسام المتماسة يتصرف بشكل لزج مرن والمادة ناعمة تصبح هذه المسائل أكثر تعقيد. في هذا البحث ، تم اقتراح نمذجة رياضية لمسائلة التماس السطح البيني وتماس السطوح المحددة اللزجة المرنة التي يمكن تطبيقها على أطراف الأصابع

الروبوتية والاصطناعية النصف اسطوانية . تضمن الانجاز الجديد من هذا البحث دمج الوقت المعتمد الطبيعي لتماس اللزج المرن في نمذجة المسك والمناولة. على وجه التحديد، تم اقترح اثنين من معادلات الاقتران لربط اثنين من المتغيرات المهمة لنمذجة التماس (نصف عرض مساحة المستطيل المتماسة ومسارتوزيع الضغط خلال تماس للسطح البيني). بالإضافة إلى ذلك، تم دراسة حالتين قابلة للتطبيق على المسك للأيدي الاصطناعية والروبوتية: مساحة التماس الثابتة والقوة العمودية الثابتة. أظهرت النتائج أن السيطرة على قوى المسك (الحالة 2) تكون اكثر فائدة عند استخدام التماس اللزج المرن، لأنه يحسن استقرارية المسك من خلال توسيع مساحة السطح المحدد مع انقضاء الزمن. أخيرا، أثبتت نتائج السطوح المحددة اللزجة المرنة أن النموذج الرياضي الجديدي أكثر فاعلية (18-22 %) من النماذج السابق

.

الكلمات المرشدة: تماس اللزج المرن ، أطراف الأصابع النصف اسطوانية ، مادة لينة ، المرونة الغير الخطي.

1. Introduction

One of great significant mechanical characteristics of fingertips is soft material [1]. Soft material contact mechanics represents a paramount role in grasping stability as well as safe object prehension and handling during manipulation [2]. Hertz first presented the modeling of contact mechanics, based on point contact between two linear elastic materials [3]. If Coulomb's friction model is used, all the forces that lie within the friction cone can be applied [4]. The employment of this contact model in the manipulation planning problem has led to some interesting conclusions. There may be multiple solutions to a particular problem (opacity), or there may be no solutions (discrepancy) [5]. Friction "limit surface" is a fictional surface within which slipping does not happen; that is, the limit surface is the boundary between non-sliding vs. sliding motions in prosthetic and robotic hands for grasping and manipulation [6]. However, robotic fingertips are manufactured from nonlinear elastic materials. For that reason, the Hertzian contact model does not strictly represent this contact. A power-law theory was deduced for modeling nonlinear elastic contacts present in robotic hand fingers by [7-9] for hemispherical and hemicylindrical soft fingertips, respectively.

Viscoelastic contact comprises, aside from linear or nonlinear elastic response, time-dependent response due to relaxation or creep phenomena that dominated the contact behavior [10]. As the materials and geometric designs of fingertips varied, the viscoelastic action of particular types of fingertips was noticed, in particular with the relaxation of fingertip contact force or the creep of contact zone, and characteristics of viscoelastic contact [11]. Applications of such contact modeling of human and biomedical fingertips were studied [12]. The viscoelastic contact of hemispherical fingertips was investigated [13]. The evolution of their friction limit surfaces and of the pressure distributions at the contact interface was studied. A quasistatic frictionless contact problem for viscoelastic bodies with long memory was considered [14] and modeled the contact with normal compliance in such a way that the penetration is limited and restricted to unilateral constraints. The adhesion between contact surfaces was taken into account, and the evolution of the bonding field was described by a first order differential equation.

It is noted that none of the above-cited references focused on the analysis of viscoelastic contact and grasping stability problems of hemicylindrical fingertips for robotic and prosthetic hands. Therefore, the aim of this research is to develop the pressure distribution and limit surfaces of a hemicylindrical soft fingertip for viscoelastic contact interface, due to its time-dependent nature, as well as the implication of such evolving limit surfaces on the stability of grasping for robotic and prosthetic hands. This research introduces a proper modeling of viscoelastic contact that can cover the analysis of contacts to satisfy the elastic and temporal responses of contacts. Finally, an analytical study will be verified for nonlinear viscoelastic characteristics of the proposed fingertip and compared with the previous model.

2. Modeling of Viscoelastic Hemicylindrical Fingertips

In general, the modeling of finger for the human and robotic hand can be solid and homogeneous, as discussed in [15] and [16], or its body can have a constant thick, soft layer covering a rigid "core," as studied in [8] and [16], see **Figure (1a-C)** . A hemicylindrical viscoelastic fingertip makes contact with a rigid flat surface by the application of a normal force N, with corresponding normal moment and tangential force at the contact interface, as shown in **Figure (1d).**

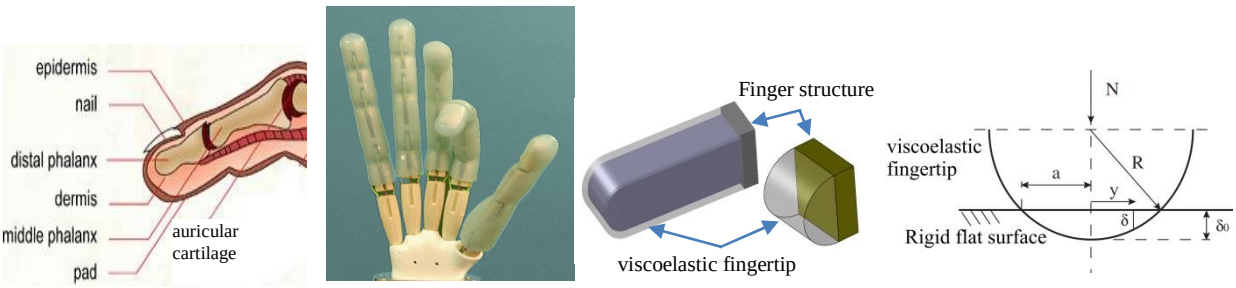

(a) **(b)** **(c)** **(d)**

Fig .(1) (a) Human fingertip. (b) Anthropomorphic fingers (c) Hemicylindrical viscoelastic fingertip with or without rigid core (d) Geometry of contact between a hemicylindrical fingertip and a rigid plane surface[15, 16, 8]

For the sake of modeling, the contact is assumed to be hold without slip; that is, the resulting tangential force and normal moment at the contact area are within the friction limit surface. From **Figure (1),** the following geometrical relationship can be written [17]:

$$a^2 = R^2 - (R - \delta)^2 \qquad (1)$$

Moreover, the following general equation of pressure distribution of hemicylindrical soft fingertip is utilized [9]:

$$P_{(y)} = C_k \frac{N}{\pi a B} \left[1 - \left(\frac{y}{a}\right)^k\right]^{\frac{1}{k}} \qquad (2)$$

where C_k is a coefficient, a function of k, that regulates the profile of pressure distribution to accept the equilibrium condition at the contact interface. Hertz [18] first presented a pressure distribution, corresponding to k = 2 in equation (2), for linear elastic contact with small deformation, which was adopted later for instance in [19], but the value for is not necessarily 2 for a general contact pressure distribution. Indeed, in a typical viscoelastic contact problems, after relaxation due to the time-dependent characteristics, the contact pressure distribution will be more uniformly, corresponding to a higher value in equation (2). Equation (2) is adopted and k is allowed to change to render different pressure distributions over the contact surface, as illustrated in **Figure (2).** Furthermore, the parameters a and N in equation (2) are not necessarily constants, due to the relaxation and creep of viscoelastic contacts. Therefore, it is significant to observe the general formulation of pressure distribution, and to recognize that the pressure distribution for viscoelastic soft fingers is a function of time.

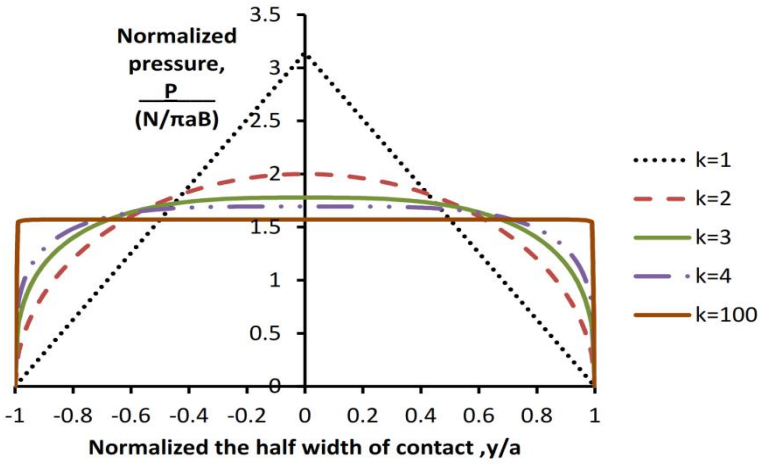

Fig .(2) Pressure distribution of Hemicylindrical viscoelastic fingertip contact depends on equation (2) [9]

Equation (2) can be integrated over total contact area A to get the coefficient C_k, and the equilibrium condition at the contact interface can be applied

$$N = \int_A P(y) \quad dA \quad = \int_{-b}^{b} \int_{-a}^{a} P(y)\, dy\, dx \qquad (3)$$

from which it is deduce that [9]

$$C_k \quad = \quad \pi \frac{k\,\Gamma\left(\frac{2}{k}\right)}{\left[\Gamma\left(\frac{1}{k}\right)\right]^2} \qquad (4)$$

Where Γ is gamma function and k is a positive real number. It is clear from equation (4) that C_k is only a function of k (see the table 1). In this work, two different cases will be studied due to the nature of the time-dependent functions for contact modeling of viscoelastic hemicylindrical fingertips. At first case, a prescribed constant contact area (i.e. constant normal displacement case) is used and the influence of relaxation is studied, as illustrated in **Figure (3a).** The second case considers the creep phenomenon due to a constant normal load, as shown in **Figure (3b).** To describe the viscoelastic behavior, a general approach considers the normal force and the displacement regarding functions as the form [20]

$$N(t) = \phi(\delta, t) \qquad (5)$$

$$\delta(t) = \psi(N, t) \qquad (6)$$

Table .(1) Values of C_k for different values of k.

k	C_k
1	3.142
2	2
3	1.778
4	1.694
6	1.630
10	1.594
100	1.5708

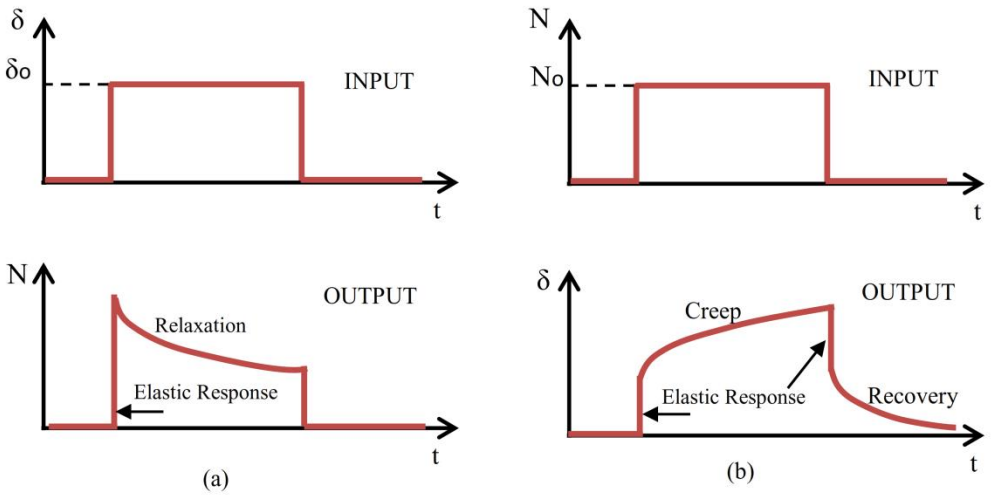

Fig .(3) (a) Case I: contact with imposed displacement (b) Case II: contact with imposed normal load. [19, 20]

that can be very complex to implementing. The function ϕ is relaxation function and the function ψ is the creep compliance. In the general case of nonlinear viscoelasticity, the relaxation function ϕ designates the force response to a step displacement δ from the undeformed shape, while the creep compliance ψ allows the displacement response to a step force from the undeformed shape. Creep and relaxation are related because of the two functions are two aspects of the same viscoelastic phenomenon [20]. When the linear hypothesis holds, the functions ϕ and ψ become only function of time and specify, respectively. Equation (5) and equation (6) will become

$$N(t) = \hat{\phi}(t) \cdot \delta \qquad (7)$$

$$\delta(t) = \hat{\psi}(t) \cdot N \qquad (8)$$

where δ is mandatory displacement at the contact, and N is the contact force. The hypothesis of Fung [21] will be used in this paper so as to overcome the complexity of the formulation equation (5) and equation (6) in the general case of nonlinear viscoelasticity. Also, the reduced relaxation function $g(t)$ and the reduced creep compliance $h(t)$will be introduced in the following sections to characterize the time-dependent behavior of viscoelastic contacts. Firstly, it should be noted that the hypothesis of Feng [21] separates the elastic response from the time response. This approach enables to utilize elastic response based on different models developed for soft fingertips, independent of the time response for viscoelastic contacts. Particularly, the viscoelastic contact modeling of soft finger can be thought of as the concatenation of the linear or nonlinear elastic response, a function of the imposed δ or N and the temporal response with creep or relaxation, a function of time.

3. Contact with imposed displacement of hemicylindrical fingertips

Figure 3(a) illustrated the first case, the hemicylindrical viscoelastic fingertip pushing onto the rectangular contact surface is considered while maintaining a constant step displacement δ_0. Relaxation phenomenon occurs and the contact force will reduce with time [19, 20] due to the viscoelastic behavior, as explain in **Figure (3a).** Because the normal displacement is held constant, the half width contact of rectangular contact area for hemicylindrical fingertips also remains constant due to the contact geometry, as given by equation (1). Due to the fact that the total normal contact force varies over time, the pressure distribution over the entire rectangular contact area changes according to the following equation by modifying from equation (2):

$$P_{(y,t)} = C_k \frac{N(t)}{\pi a B} \left[1 - \left(\frac{y}{a}\right)^k\right]^{\frac{1}{k}} \quad (9)$$

where the normal force $N(t)$ becomes time-dependent because the contact displacement and half width contact of rectangular contact area do not change, while the parameters $a, B, k,$ and C_k remain constant as in equation (2). Also, the shape of the pressure distribution is assumed constant. To model the relaxation of normal force N after the contact is made, and in order to overcome the difficulties of formulation in equation (5), the noticeable model suggested by Fung [21] for the tissues of human and used by [22, 23] to model the human fingertip behavior is adopted. The relaxation-function (ϕ) was assumed by Fung [21] as the following equation

$$\phi(\delta, t) = N^{(e)}(\delta) \,.\, g(t) \qquad with\ g(0) = 1 \quad (10)$$

where $N^{(e)}(\delta)$ is the elastic response, with superscript "(e)" denoting the elastic response, and $g(t)$ is the reduced relaxation function which characterizes the time-dependent behavior of the material. A quasi-linear viscoelastic model has been improved by [24, 25]. The term $N^{(e)}(\delta)$ is the amplitude of the force generated promptly by a displacement from the undeformed configuration. The nonlinear elastic response $N^{(e)}$can be modeled through several analytical expressions. Two important models of the elastic stiffness $K^{(e)}(\delta) = {dN}/{d\delta}$ used in the literature are

$$K^{(e)}(\delta) = m \,.\, e^{w\delta} \quad (11)$$

$$K^{(e)}(\delta) = p.\delta^q \quad (12)$$

where (m, w) and (p, q) are parameters which depend on the geometry and materials. The expression of can be found from equation (11) or equation (12) after the integration them with respect to δ, as well as the initial condition $N^{(e)}|_{\delta=0} = 0$

$$N^{(e)} = \frac{m}{w}\left(e^{w\delta} - 1\right) \tag{13}$$

$$N^{(e)} = \frac{p}{q+1}\delta^{q+1} \tag{14}$$

Equation (11) was utilized by Pawluk and Howe [22] and Barbagli et al. [26] to model the relationship between normal force and normal displacement in human finger indentation. The human finger stiffness was compared with that of artificial fingers using both equations (11) and (12) by Han and Kawamura [27]. Kao and Yang [17, 28], beginning from previous research results [8], deduced an expression for nonlinear stiffness of soft contact that can be related with equation (12). Tiezzi and Vassura [29] utilized both equations (11) and (12) to inspect the behavior of elastic skins covering a rigid fingertip structure. The reduced relaxation function $g(t)$ is a time-decaying function. When normalized to 1 $at\ t = 0$, it can be illustrated by the following equation [20, 22]:

$$g(t) = \sum_{i=0}^{n} c_i\ e^{-v_i .t} \quad \text{with} \quad \sum_{i=0}^{n} c_i = 1 \ \text{and}\ v_0 = 0 \tag{15}$$

where the parameters c_i and v_i be depended on the material of the viscoelastic interface, and the exponents match the rates of the relaxation phenomena. The relaxation function ϕ , explained in equation (10), knows the force response to a step displacement δ from the undeformed configuration as time elapses. Thus, in the case of a single step displacement $\delta = \delta_0$, the force response will be

$$N(t) = N^{(e)}(\delta_0)\ .\ g(t) \tag{16}$$

The pressure distribution at the contact interface of the viscoelastic fingertip is found by substituting equations (15) and (16) into equation (9) to obtain the following equation

$$P_{(y,t)} = \frac{C_k}{\pi a B}\left[1 - \left(\frac{y}{a}\right)^k\right]^{\frac{1}{k}}\left[c_0 + \sum_{i=1}^{n} c_i\ e^{-v_i .(t-\tau)}\right] N^{(e)}(\delta_0) \tag{17}$$

The first part in equation (17) depends only on y , while the second term expresses the time dependence of the pressure distribution due to the variation normal force $N(t)$. **Figure**

(4) explains the calculated results of the pressure distribution of hemicylindrical fingertips due to the relaxation of the normal force in the case of a constant normal displacement $\delta_0$with a second-order contact pressure distribution profile $(k = 2)$. In order to display only the relaxation state, **Figure (4 A,B)** plots the normalized force N/N_0 and pressure P/P_0, respectively. The parameters of the decreased relaxation function $g(t)$, used to plot the graphics, are $n = 1, c_0 = 0.7, c_1 = 0.3$ and $v_1 = 3.1$ which are concluded from the experimental results mention in [24, 25].

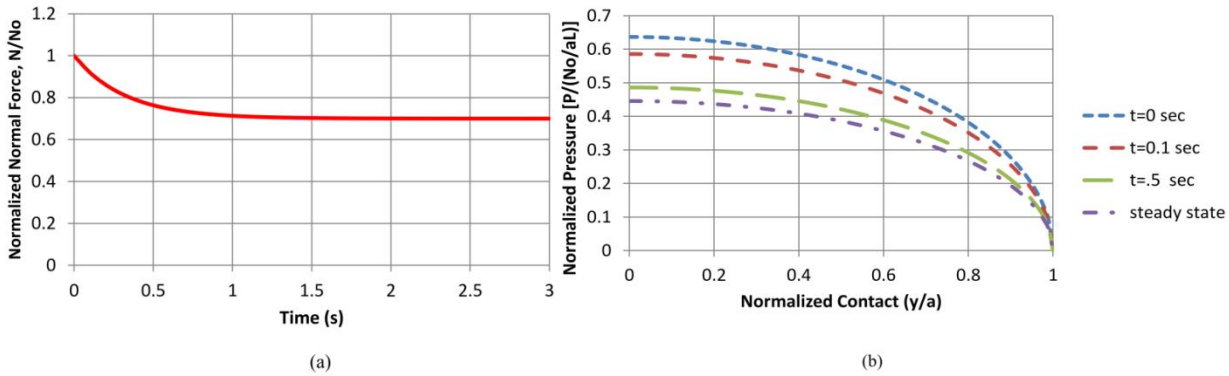

Fig .(4) (a) Relaxation of normal load when a constant normal displacement is imposed. (b) Evolution of the pressure distribution due to the relaxation of the normal load using $k = 2, C_k = 2, c_0 = 0.7; c_1 = 0.3, \text{and } v = 3.1$.

If the imposed displacement of hemicylindrical fingertip is changing, the contribution of the whole past history should be taken into consideration. The normal force resulted by an infinitesimal displacement $d\delta(\tau)$, superposed in a condition of displacement of hemicylindrical fingertip at an instant of time τ, with $t > \tau$, is

$$dN(t) = g(t-\tau)\ \frac{dN^{(e)}(\delta(\tau))}{d\delta}\ d\delta(\tau) \qquad (18)$$

as deduced from equation (16). By using a modified superposition principle [20, 30, 31], the total normal force at the time instant is the sum of contribution of all the past changes; that is

$$N(t) = \int_0^t g(t-\tau)\ \frac{dN^{(e)}(\delta(\tau))}{d\delta}\ \frac{d\delta(\tau)}{d\tau}\ d\tau \qquad (19)$$

Equation (19) will be rewritten as follows:

$$N(t) = \int_0^t g(t-\tau).K^{(e)}(\delta(\tau))\ .\ \dot{\delta}(\tau)\, d(\tau) \qquad (20)$$

where $K^{(e)}$ is the elastic stiffness as indicted by equations (11) or (12), and $\dot{\delta}(\tau)$ is the rate of hemicylindrical fingertip displacement. The evolution of the pressure distribution is found by substituting equations (15) and (20) into equation (9). That is

$$P_{(y,t)} = \frac{C_k}{\pi a B}\left[1-\left(\frac{y}{a}\right)^k\right]^{\frac{1}{k}} \int_0^t \left[c_0 + \sum_{i=1}^{n} c_i\, e^{-v_i.(t-\tau)}\right] . K^{(e)}(\delta(\tau)) .\ \dot{\delta}(\tau)\, d(\tau) \qquad (21)$$

4. Contact with imposed normal load on the hemicylindrical soft fingertip

For the case in which the normal load ($N = N_0$) applied on the hemicylindrical soft fingertip is maintained at constant, the normal displacement δ will increase over time because of the nature of viscoelastic creep phenomena [20], as illustrated in **Figure (3b).** Moreover, it is well known that by conservation the normal force constant, the pressure distribution of viscoelastic contact will gradually become more uniform because of relaxation [19, 32]. Indeed, as a result of the increasing normal displacement, the half width of contact area a also increases, while the depth 2b remaining nearly constant that proved by experimental by [8, 17], while, the equilibrium condition at the contact area imposes a constraint equation with the normal force N being constant, as in equation (3). The shape of pressure distribution changes because the rectangular contact area increases while the normal force is held constant, implying the changes in the shape factor of pressure profile k in equation (2). The pressure distributions for various typical values of N and a are plotted in **Figure (2).** In the following modified pressure distribution equation (22) which a and k are functions of the time

$$P_{(y,t)} = C_{k(t)} \frac{N(t)}{\pi a_{(t)} B}\left[1-\left(\frac{y}{a_{(t)}}\right)^{k(t)}\right]^{\frac{1}{k(t)}} \qquad (22)$$

where $C_{k(t)}$ indicates the coefficient C_k as a function of $k(t)$. The maximum pressure become at $y = 0$, and is found by

$$P_{max(t)} = P_{(0,t)} = C_{k(t)} \frac{N}{\pi a B} \qquad (23)$$

From equation (23), the maximum pressure decreases while the contact area increases. In **Figure (2),** the normalized maximum pressure at $y = 0$ coincides to the coefficient at each value of k. The total area under each half-curve is unity, as denoted in (24). Note that as $k \to \infty$, the pressure becomes uniformly distributed, as foreseeable. Substituting equation (22) into (3), the integral constrain equation becomes

$$\frac{C_{k(t)}}{\pi a(t)} \int_{-a(t)}^{a(t)} \left[1-\left(\frac{y}{a_{(t)}}\right)^{k(t)}\right]^{\frac{1}{k(t)}} dy = 1 \qquad (24)$$

A. Half width of contact area and pressure distribution

The constraint equation in equation (24), when integrated, will yield equation (4), which does not include $a(t)$ at any instant t. This is owing to the specific formula of contact pressure distribution utilized in equation (2). This has deep implication on the analysis of contact and the behavior of viscoelastic fingertips. The following observations are recorded.

- Theoretically, the shape factor of pressure profile k can be selected independent of the constraint equation in equation (24). The choice of k is primarily determined by the shape of the pressure distribution at the contact area. Larger value of k denotes more uniform pressure distribution
- The constraint equation (24), when integrated, does not yield an equation which retains the half width contact of rectangular contact area a. Therefore, the parameter a is independent of the equilibrium condition clarified by equation (24).
- • Due to the specific form of the contact pressure distribution, the equilibrium condition equation (24) imposes a value of C_k, clarified by equation (4), that relates the $P_{max(t)} = P_{(0,t)}$ and the mean-pressure $\frac{N}{2aB}$, taking into account the pressure distribution due to exponent k.

Although the two important parameters, half width contact of rectangular contact area a and the shape factor of pressure profile k, are independent based on the theoretical modeling as proposed here, it is postulated that the two parameters a and k are correlated, according to the properties of the fingertip geometric configuration as well as the material of the fingertip. It is useful to deduce a coupling equation for the two important parameters, in order to facilitate the analysis and formulation for the modeling of viscoelastic contact area. Such a coupling equation needs to agreement the equation equilibrium and physical coherent behavior. In the following parts, two such coupling equations are introduced and discussed.

B. Coupling equation based on pressure distribution

In this paragraph, a coupling equation based on the evolution of the profile of pressure distribution at the rectangular contact interface is derived. The fact that as the relaxation is happening, so as to set the parameters a and k . The pressure distribution becomes more uniform with gradually increasing and the half width contact of rectangular contact area enlarge too [32], as illustrate in **Figure (2).** In order to correlate the two parameters a and k , the half width contact of rectangular contact area for hemicylindrical fingertips a in such a way that is selection

$$a \propto \frac{1}{\sqrt{C_k}} \qquad (25)$$

As mentioned in Section 4-A, the coupling equation requires satisfying the equilibrium equation and physical coherent behavior. It is significant to observe that the assumption of relationship in equation (25) fulfills such criteria. Moreover, the assumptions in equation (25) give a growing half width contact of rectangular contact area when the value of diminution due to a more uniform pressure distribution. Thus, this relationship is convenient with the well-known physical behavior. The curve of k with respect to a can be plot and fit it with a weighted least-squares (LS) best fit using Matlab program [33] , based on the option of the half width contact described in equation (25), to get the following equation

$$\frac{a}{a_o} \cong c(1 - 0.52e^{-0.535k}) \qquad (26)$$

where a_o is the half width contact of rectangular contact area at $t = 0$ when $k = 2$, and $c = 1.217$, a constant. Equation (26) includes changes in contact pressure distribution corresponding to $2 \leq k \leq 6.5$ as time changes from $0 \leq t \leq \infty$. A few values of k between 2 and 6.5 with corresponding values of growing normalized half width contact are listed from **Table 2. Figure (5)** explains the growth of contact pressures and areas as time elapses that is obtained using equation (26), where the relaxation of the viscoelastic fingertip with constant normal force outcomes in the flattening of the pressure distribution at the contact area, also the increase of half width contact of rectangular contact area. The results are in line with the physical behavior of viscoelastic contacts [32].

Table .(2) Values of C_k and a/a_o corresponding to different values of the parameter k between 2 and 4.

k	C_k	$1/\sqrt{C_k}$	a/a_o
2	2	0.707107	0.99993
2.5	1.858	0.73363	1.050879
3	1.778	0.749953	1.089869
3.5	1.728	0.760726	1.119708
4	1.694	0.768322	1.142543
4.5	1.671	0.773592	1.160019
5	1.653	0.777792	1.173393
5.5	1.640	0.780869	1.183628
6	1.630	0.78326	1.191461
6.5	1.622	0.78519	1.197455

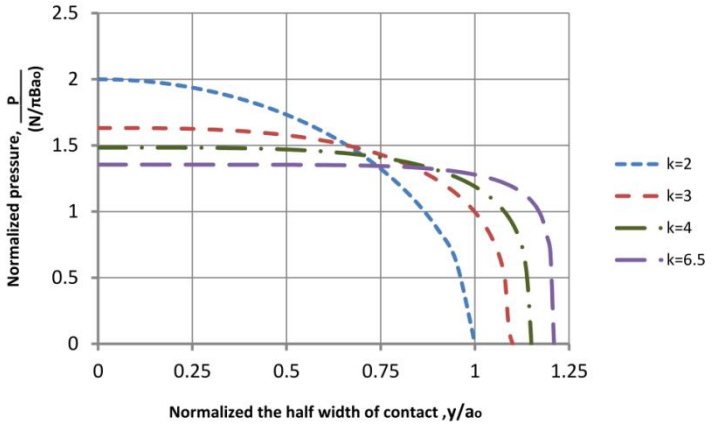

Fig .(5) Evolution of pressure distribution for the viscoelastic soft finger when the normal contact force is maintained at constant, resulting in the relaxation and growth of the half width of rectangular contact.

C. Coupling equation based on creep compliance

An alternative approach is introduced in this section based on the creep compliance to get a relationship between the parameters a and k. A constitutive equation is presented to relate both parameters with the viscoelastic property of the fingertip material. The creep compliance $\psi\,(N,t)$ is supposed to be in the form by using the same modeling approach as that in Section3:

$$\psi\,(N,t) = \delta^{(e)}(N)\,.\,h(t) \qquad with \quad h(0) = 1 \tag{27}$$

where the function $\mathrm{h(t)}$ is the reduced creep compliance that characterizes the time-dependent behavior of the fingertip, and $\delta^{(e)}(N)$ denotes the elastic response that is created by the force from the undeformed configuration.

The elastic displacement equations are found by inverting equations (13) and (14)

$$\delta^{(e)}(N) = \frac{1}{b}\ ln\left(\frac{b}{m}N + 1\right) \tag{28}$$

$$\delta^{(e)}(N) = \left(\frac{q+1}{p}\ N\right)^{\frac{1}{q+1}} \tag{29}$$

The reduced creep compliance can be explained, without loss of generality [20], by the following form:

$$h(t) = 1 + \sum_{i=1}^{n} c_i \left(e^{-\eta_i \cdot t} \right) \quad (30)$$

where the parameters c_i and η_i are constants depending on the materials, and the exponents η_i represent the rates of creep phenomena. The displacement response $\delta(t)$ is obtained from the creep compliance $\psi(N,t)$ in equation (27), which results from a single step of normal load ($N = N_0$) that is using at the initial instant $t = 0$, that is

$$\delta(t) = \delta^{(e)}(N_0) \, . h(t) \quad (31)$$

The half width contact of rectangular contact area increases because of the increase of the normal displacement. For simplicity, the relationship between the half width contact of rectangular contact area a and the displacement δ can be deduced from equation (1) as

$$a^2 \cong 2R\delta \quad (32)$$

by cancelling the second-order term in δ^2 [17]. The half width contact of rectangular contact area found from the approximation in equation (32) is slightly larger than that from equation (1). Nevertheless, the half width contact given by equation (32) is closer to the actual half width contact that is impacted by the enlargement because of the conservation of the volume of the pad at the contact interface. Substituting equation (31) into (32), to get

$$a^2(t) \cong 2R\delta(t) = 2R\delta^{(e)}(N_0) \, . \, h(t) \quad (33)$$

Equation (33) can be rewritten as

$$a(t) \cong a_o \sqrt{h(t)} \quad (34)$$

where $a_o = 2R\delta^{(e)}(N_0)$ is the half width of rectangular contact area at the initial instant. A useful hypothesis, assumed in equation (25), is $C_k \propto \frac{1}{a^2}$. Combining equation (34) with equation (34), to obtain

$$C_k \propto \frac{1}{a^2} \propto \frac{1}{h(t)} \quad (35)$$

Subsequently, it can relate the coefficient C_k and the reduced creep compliance h as follows:

$$C_k = \pi \frac{k\,\Gamma\left(\frac{2}{k}\right)}{\left[\Gamma\left(\frac{1}{k}\right)\right]^2} = \frac{C_{k0}}{h(t)} \qquad (36)$$

where $C_{k0} = C_k(k|_{t=0})$ is used because $h|_{t=0} = 1$. For example, when the initial pressure profile is second-order, i.e., $k|_{t=0} = 2$, the corresponding worth for $C_{k0}$is 1.5. The relationship between the shape factor of pressure profile k and the time can be found from equation (36). The direct use of equation (36) is not proper because the shape factor of pressure profile k is included in the arguments of the gamma function, thus an equivalent relationship between C_k and k requires to be obtained. It can be noted that the two amounts $\log(C_k - 1)$ and $\log(k)$ are linearly related, as illustrated in **Figure (6a).** By using the LS best fit, the following approximate relationship can be written as follows:

$$\log(C_k - 1) = a_1 \log(k) + 2 \qquad (37)$$

with $a_1 = -0.5261$ and $a_1 = -0.3647$. After some mathematical processing, it can be derived that the approximate relationship between the coefficient of pressure distribution over the contact area C_k and shape factor of the pressure profile k can be written as

$$C_k \cong e^{a_2} . e^{a_2 \log(k)} + 1 \qquad (38)$$

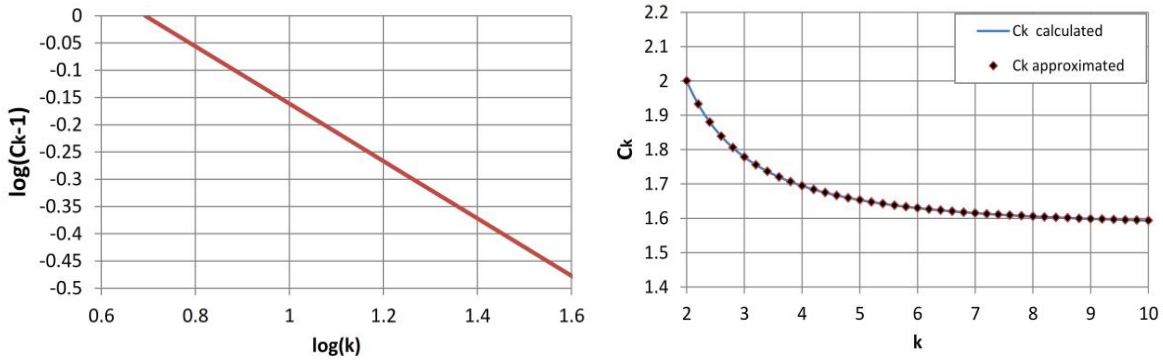

Fig .(6) (a) Linear relationship between $\log(k)$ and $\log(C_k - 1)$ is plotted. (b) Comparison between the calculated and approximated C_k values in equation (38).

Equation (38) is a very good approximation of $C_k(k)$ over a larger range of k, as shown in **Figure 6 (B),** where the constants a_1 and a_2 are found through the LS method. Substituting equation (38) into equation (36), to obtain

$$\alpha_2 \cdot e^{\alpha_1 \log(k)} + 1 = \frac{C_{k0}}{h(t)} \quad (39)$$

Where $\alpha_1 = a_1$ and $\alpha_2 = e^{a_2}$, therefore the alteration of k as a function of time can be found from equation (39), that is

$$K_{(t)} = \left[\frac{\frac{C_{ko}}{h(t)} - 1}{\alpha}\right]^{\beta} = \left[\frac{\frac{C_{ko}}{h(t)} - 1}{1.44}\right]^{-1.9} \quad (40)$$

where $\alpha = \alpha_2 = 1.44$ and $\beta = \alpha_1^{-1} = -1.9$. Equation (40) appears that the relationship between K and time is only impacted by the properties of the material through the reduced creep compliance. **Figure (7)** explains C_k as a function of k, as explained by equation (4), and K as a function of time, as explained by equation (40). The function $h(t)$ is supposed to be in the form of equation (30) with only two parameters as follow:

$$h(t) = 1 + c_1 (1 - e^{-\eta_1 \cdot t}) \quad (41)$$

where $c_1 = 0.3$ and $\eta_1 = 3.1$. This option is proper with the experimental results that are obtained from [24, 25].

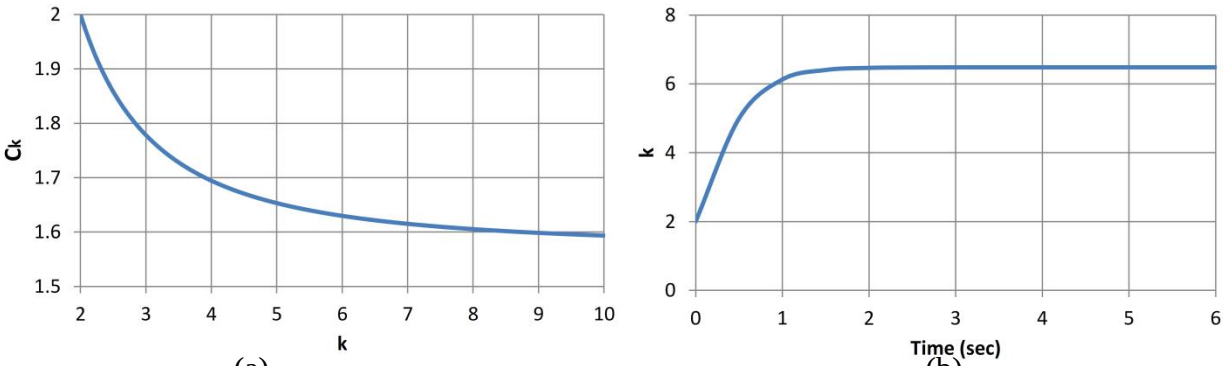

(a) (b)

Fig .(7) (a) Plot of C_k as a function of k, as shown by equation (4). (b) Plot of k as a function of time, as illustrated by equation (40), by adopting reduced creep compliance $h(t)$, as expressed by (41).

The pressure distribution $P_{(y,t)}$ can be obtained by substituting equations (34), (40), and (41) into (22). **Figure (8)** shows the results of the creep of the viscoelastic fingertip by keeping the normal force constant as well as the evolution of the half width contact, resulting in the flattening of the pressure distribution at the contact. The resulting relaxation and growth

of the contact area are exponential because of the option of the reduced creep compliance (41). As over time, the pressure distribution approaches a more constant profile, with k varying from 2 to 6.46 (as shown in figure 7) and the half width contact of rectangular contact area is heighten by approximately 11%. In general, the contribution of the whole past history must be considered when the normal load N is not constant but varying. To drive the dual relationship of equation (19) by substituting $N^{(e)}(\delta)$ with $\delta^{(e)}(N)$ and $g(t)$ with $h(t)$ similar to section 3 is adopted. Consequently, the change of the normal displacement δ as a function of time can be shows as

$$\delta(t) = \int_0^t h(t-\tau) \frac{d\delta^{(e)}(N(\tau))}{dN} \frac{dN(\tau)}{d(\tau)} d(\tau) \quad (42)$$

Or

$$\delta(t) = \int_0^t h(t-\tau) C^{(e)}(N(\tau)) \dot{N}(\tau) d(\tau) \quad (43)$$

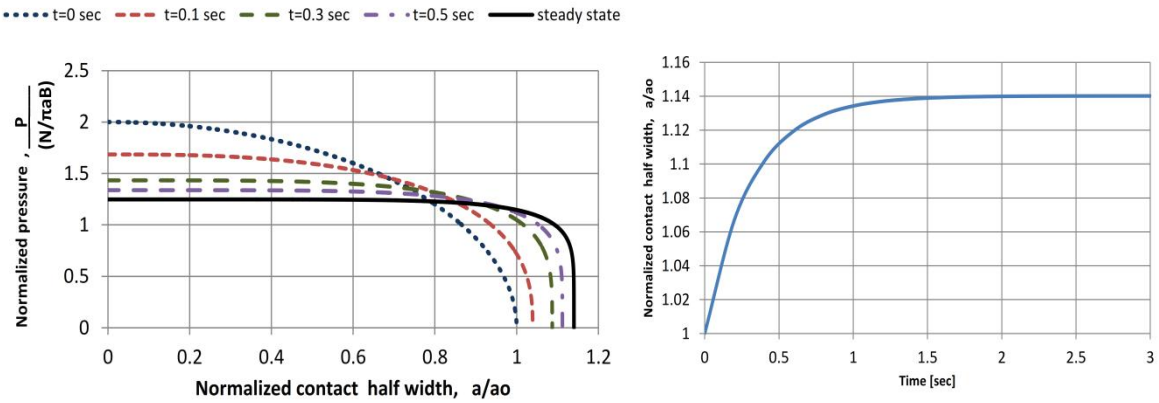

(a) (b)

Fig .(8) (a) The pressure distribution as a function of the normalized half width contact of rectangular contact area a/a_0 (b) The half width contact of rectangular contact area as a function of time.

where $C^{(e)}$ is the elastic compliance, and $\dot{N}(\tau)$is the rate of change of the normal contact load. The elastic compliance term is the inverse of the elastic stiffness $K^{(e)}$

$$C^{(e)} = \frac{d\delta^{(e)}}{dN} = \frac{1}{K^{(e)}} \quad (44)$$

from equations (13) and (14), to obtain

$$C^{(e)}(N) = \frac{1}{bN + m} \tag{45}$$

$$\delta^{(e)}(N) = \frac{1}{p}\left(\frac{q+1}{q}\ N\right)^{\frac{-q}{q+1}} \tag{46}$$

Subsequently, the half width contact of rectangular contact area becomes a function of the normal load history, as illustrated by the following equation:

$$a^2(t) = 2R\int_0^t h(t-\tau)\quad C^{(e)}\big(N(\tau)\big)\quad \dot{N}(\tau)\ d(\tau) \tag{47}$$

which is found by substituting equation (43) into equation (32). Likewise, the parameter $k(t)$ becomes a function of the normal load history as showed in equation (40). Therefore, this is the convolution integral, that is

$$\int_0^t h(t-\tau)\,.\quad C^{(e)}\big(N(\tau)\big)\,.\quad \dot{N}(\tau)\ d(\tau) \tag{48}$$

Also, the pressure distribution in equation (22) becomes a function of the normal load history.

5. Construction of limit surfaces in viscoelastic of hemicylindrical fingertips

In this section, the construction of the limit surfaces depended on the theoretical models of the two cases introduced in the preceding sections is considered. The basics of the limit surface construction are illustrated in Appendix. The new achievement of this research is to adopt the methodology to explain the evolution of limit surfaces in viscoelastic contacts of hemicylindrical fingertips. The evolution of limit surfaces as a time-dependent feature of typical viscoelastic contact interface is introduced and discussed.

a. Constant rectangular contact area

The construction of limit surface in the case of constant rectangular contact area is similar to that of an elastic fingertip in contact. The details can be seen in Appendix. The integrands in equation (A5) and equation (A6) do not depend on time, and are particularly the same of the elastic soft fingertips in contact. The two equations proposed that the friction limit surfaces are developed, based on the changing normal force $\mathrm{N(t)}$, with the shape of each

individual limit surface being the same as that of the corresponding limit surface for elastic soft fingertip at the same normal force at each time instant. In the current case, the shape of the limit surface does not change, but scales proportionally inward as N decrease. If the normal force reduces exponentially, as seen in figure 4(a), both the tangential force and the moment will also reduce exponentially. The normalized tangential force and normal moment can be explained as follows from equations (A5) and (A6) for the construction of the limit surface:

$$\frac{f_t(t)}{\mu N(t)} = \frac{C_k}{2\pi} \int_{-1}^{1}\int_{-1}^{1} \frac{(\tilde{x} - \tilde{d}_c)}{\sqrt{(\tilde{x} - \tilde{d}_c)^2 + (\tilde{y} * D)^2}} \; (1 - \tilde{y}^k)^{\frac{1}{k}} \; d\tilde{y}\, d\tilde{x} \qquad (49)$$

$$\frac{m_z(t)}{\mu a N(t)} = \frac{C_k}{2\pi} \int_{-1}^{1}\int_{-1}^{1} \frac{(\tilde{x}^2 - \tilde{x}\tilde{d}_c + (\tilde{y} * D)^2)}{\sqrt{(\tilde{x} - \tilde{d}_c)^2 + (\tilde{y} * D)^2}} \; \frac{1}{D} \; (1 - \tilde{y}^k)^{\frac{1}{k}} \; d\tilde{y}\, d\tilde{x} \qquad (50)$$

where the normalized coordinates $\tilde{y} = \frac{y}{a}$, $\tilde{d}_c = \frac{d_c}{b}$, and $\tilde{x} = \frac{x}{b}$ are used to make easy the integration processes. Since the normal force reduces exponentially and approaches asymptotically a specific value after a certain settling time, as illustrated in figure 4(a), the change of limit surface will follow the same exponential pattern. An example of the evolution of such limit surfaces in the first quadrant is plotted in **Figure (9)** by imposing that the pressure distribution and coefficient C_k do not change. As illustrated in **Figure (9**), the limit surfaces move inward as the normal force $N(t)$ reduces. The exponential decay proposes larger shrinkage initially, while asymptotically approaches a constant surface as $t \to \infty$.

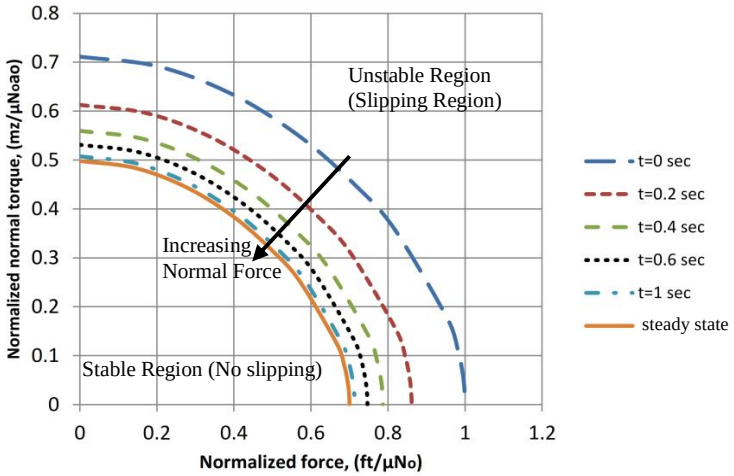

Fig .(9) Limit surface when the contact area is continued at constant to the decay of normal force from N_0 to N_f.

b. Constant normal load

As researched in Section 4, when the normal contact force is maintained constant ($N = N_0$), the normal displacement and half width contact will gradually relax as time elapses. By using the equations obtained in Section 4-C and substituting equation (22) into equations (A1) and (A3), the normalized force and moment for the viscoelastic contact of hemicylindrical fingertip can be formulated, similar to equations (A5) and (A6), as illustrated in equations (51) and (52), where $\tilde{y} = \frac{y}{a_0}$, $\tilde{d}_c = \frac{d_c}{b}$, $\tilde{a} = \frac{a}{a_0}$, $D = \frac{a}{b}$, and $\tilde{x} = \frac{x}{b}$ are the normalized coordinates, and the parameters $a(t)$, $k(t)$, and $h(t)$ evolve as prescribed in equations (34), (40), and (41). The limit surface can be found by using these two equations, but the evolution of the limit surfaces as time elapses is less axiomatically. The results of integration of equations (51) and (52) in **Figure (10)** are showed. The development of the limit surfaces when time elapses can be explained from the figure as they move outward.

$$\frac{f_t(t)}{\mu N_0} = \frac{1}{2\pi} \int_{-1}^{1} \int_{-\tilde{a}}^{\tilde{a}} \frac{(\tilde{x} - \tilde{d}_c)}{\sqrt{(\tilde{x} - \tilde{d}_c)^2 + (\tilde{y} * D)^2}} \left(1 - (\frac{\tilde{y}}{\tilde{a}})^{k(t)}\right)^{\frac{1}{k(t)}} \frac{C_{k(t)}}{\tilde{a}} \, d\tilde{y} \, d\tilde{x} \qquad (51)$$

$$\frac{m_z(t)}{\mu a_0 N(t)} = \frac{C_k}{2\pi} \int_{-1}^{1} \int_{-\tilde{a}}^{\tilde{a}} \frac{(\tilde{x}^2 - \tilde{x}\tilde{d}_c + (\tilde{y} * D)^2)}{\sqrt{(\tilde{x} - \tilde{d}_c)^2 + (\tilde{y} * D)^2}} \frac{C_{k(t)}}{D * \tilde{a}} (1 - \tilde{y}^k)^{\frac{1}{k}} \, d\tilde{y} \, d\tilde{x} \qquad (52)$$

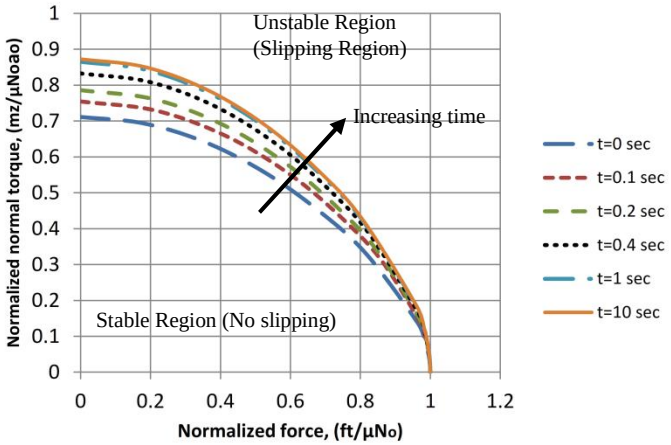

Fig .(10) The limit surface as a function of time in the case of constant force.

6. Verification the present model

To verify the importance of the new model adopted in the current research, the hemicylindrical soft fingertips are applied to the viscoelastic limit surfaces based on the theoretical models of the two cases presented in the preceding sections, which are based on the current theoretical proposed, are compared with other results obtained by the earlier investigators [13] for viscoelastic contact of the hemispherical soft fingertip at same radius of fingertip, shape factor of the pressure profile, and applied load, and conditions. **Figure (11.a)** shows sample result of limit surface when the contact area is maintained constant, in which the constant half width contact of rectangular contact area for hemicylindrical fingertip is remained, resulting in the exponential decrease of the normal force. The limit surface will also scale in proportion to the decay of normal force from N_0 to N_f ,while **Figure (11.B)** shows sample result hemispherical soft fingertip [13] at same conditions. Development of the limit surface for the present work, as a function of time in the case of constant normal force, is shown in **Figure (12.A).** The tangential force f_t is normalized with respect to the maximum tangential force at the instant $t = 0$, and the normal moment m_z is normalized with respect to the product $\mu a_0 N_0$. And, **Figure (12.B)** presents sample result hemispherical soft fingertip [13] at same conditions. The results showed that viscoelastic limit surfaces have been enhanced (18 - 22 %), if hemicylindrical fingertips are utilized instead of hemispherical fingertips at the same radius of fingertip, shape factor of the pressure profile, and applied load. Despite the similarity relative to the shape of results of the two models because both models were adopted on the same principle in the assumption and approach to get viscoelastic contact interface for soft fingertips, but they differ in the shape of contact area that effects on magnitude of pressure distribution across the contact interface as well as the application of such evolving viscoelastic limit surfaces. Moreover, the half width contact of the hemicylindrical fingertip can be controlled easily, in the case of hemicylindrical fingertip, by altering the depth of the hemicylinder, while this is limited in the case of hemispherical tip due to axis symmetry.

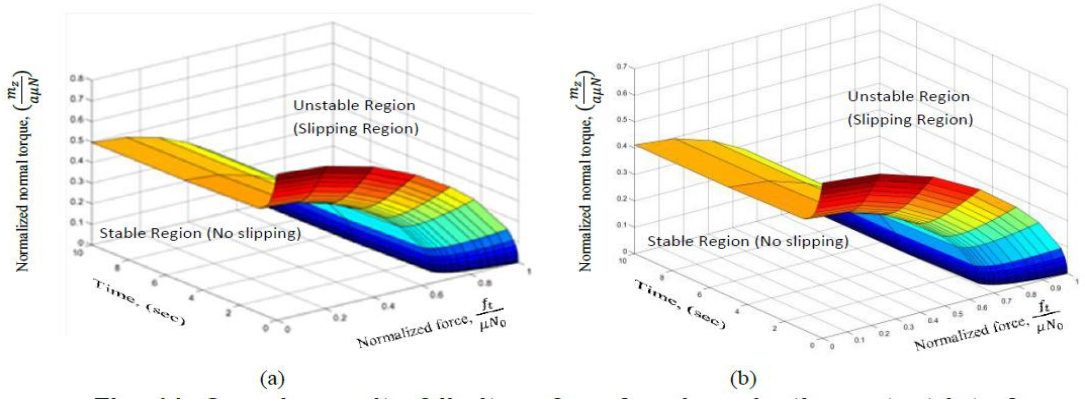

Fig .(11) Sample result of limit surface for viscoelastic contact interface when the contact area is maintained at constant, in which (a) the constant half width of rectangular contact is maintained (present work), (b) the constant radius of circular contact is maintained [13].

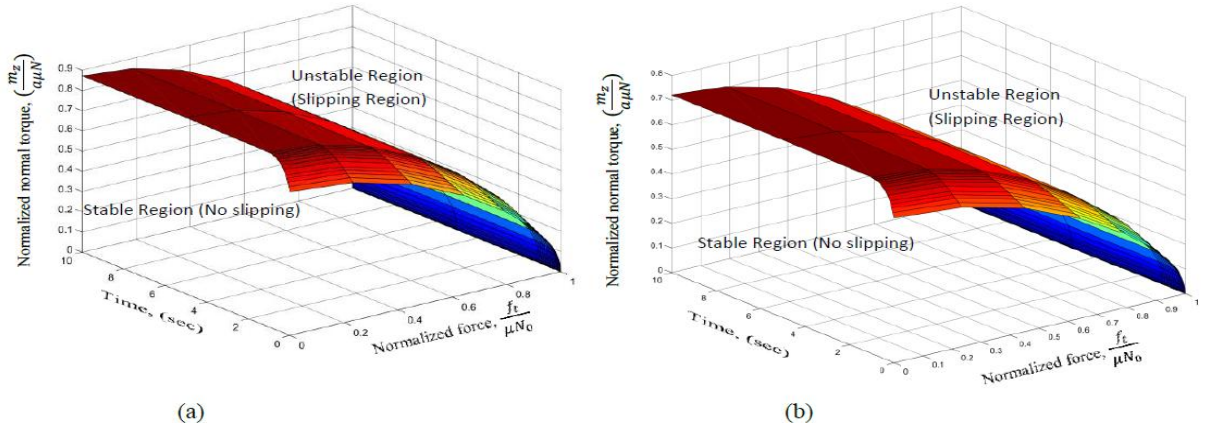

Fig .(12) The limit surface as a function of time in the case of constant normal force. (i. e. $N_0 = const.$). The tangential force f_t is normalized with respect to the maximum tangential force μN_0 at the instant $t = 0$, and the normal moment m_z is normalized with respect to the product $\mu N_0 a_0$, (a) Hemicylindrical soft fingertips (present work). (b) Hemispherical soft fingertips [13].

7. Discussions

The viscoelastic contact models for hemicylindrical soft fingertips introduced in this research are depended on separating the effects of the instantaneous time-independent elastic response and the time-dependent creep or relaxation response. The suggested approach has been explained to be very beneficial, because the model can be found by utilizing elastic modeling previously developed. Recent researches in contact with inclined hemicylindrical soft fingertips were introduced in [34-36] using elastic modulus of fingertip and stiffness model in conjunction with geometry. Such researches and previous modeling of soft fingers [1, 7-9, 27, 28, 37] study the elastic response in contacts of grasping and manipulating. Such models give augment to the elastic response as illustrated by $N^{(e)}(\delta)$. Viscoelastic modeling can utilize any of such modeling to get the elastic response of hemicylindrical soft fingertips and raise it with the temporal response. Using the present model, the temporal response and the elastic response can be separated and dealt with independently. By the kind of the modeling equations, the two necessary parameters governing the contact (namely, the half width contact a and the shape factor of pressure profile n at the contact interface) are not directly related by employing the modeling and analytical equations. Moreover, coupling equations are suggested to correlate the two parameters based on pressure distribution and creep compliance. The former is valuable when $2 \leq k \leq 6.5$, while the other is more general for all ranges of k values. It is shown that both equations satisfy the equilibrium equation and physical coherent behavior of viscoelastic contacts. The reduced creep compliance $h(t)$ is presented, which functions only on the viscous properties of the material, for the modeling of

the creep behavior at the contact interface. By using this function, the evolution of both the pressure distribution, depending on k, and the half width contact of rectangular contact area a, can be obtained. A noticeable is conclusion that both parameters k and a are related to the same function h(t). Furthermore, they relied on the geometry.

Two cases are presented with respective modeling equations and introduced with the evolution of limit surfaces as time elapses. The two cases are constant rectangular contact area and constant normal force. In the first case with constant contact deformation, and thus constant contact half width of rectangular contact area, it is obtained that the relaxation and reduction of normal force makes the limit surfaces shrink asymptotically, resulting in a less stable grasp because its viscoelastic behavior. This is explained in **Figure (9).** In the second case with constant normal force, the contact area augments due to creep. As a result of the growth of the rectangular contact area while maintaining the same normal force, the limit surface increases, promoting the stability of grasping at the contact interface. This is clarified in **Figure (10),** in which the limit surfaces alter the shapes because the maximum tangential force (when $m_z = 0$) relies only on the normal load and the friction coefficient, but does not depend on the viscoelastic phenomena. Furthermore, the maximum normal moment augments, because the contact area enlarges and the pressure distribution becomes more uniform. Since the normal to the limit surface appears the instantaneous direction of sliding, this result also has a deep inclusion on the grasping and manipulation using viscoelastic fingertips. In typical grasping tasks, a normal force is kept and dominated instead of the contact deformation. Based on the former discussions, it is deduced that such grasp with viscoelastic contacts will become more stable as time elapses because of the time-dependent nature of viscoelasticity, as illustrated in **Figure 10**. While this is intuitive, the viscoelastic modeling introduced in this study shows such an intuition.

Thus, robotic and prosthetic fingertips presented with soft materials that display notable viscoelastic behavior are more valuable, because the relaxation phenomena create and an advanced growth of rectangular contact area under the same normal loads occurs, resulting in expanded limit surface and increased stability against sliding at the contact interface. However, it is noted that manipulation without detailed contact modeling was introduced in [38-41] with regard to sensor less manipulation. This research introduces a proper modeling of viscoelastic contact that can cover the analysis of contacts to satisfy the elastic and temporal responses of contacts. Such modeling, when achieved, will enhance the ability in grasping and manipulation by adopting the features of contacts.

8. Conclusions

This research clarifies the effect of the time-dependent relaxation nature of viscoelastic hemicylindrical soft fingertips in contact interface for robotic and prosthetic grasping. The principle of splitting between the elastic and transient responses is applied for modeling and analysis, because the time-dependent nature of the viscoelastic finger is generally independent

of the elastic response. It is concluded, when analyzing the theoretical model, that the two important parameters characterizing the viscoelastic contacts (i.e., the half width contact of rectangular contact area a and shape factor of pressure profile k) can be correlated depending on the characteristics of the materials and the physical behavior of the contact interface. Two different cases usable to robotic and prosthetic hands for grasping were studied: constant rectangular contact area and constant normal force. The development of friction limit surfaces and pressure distributions of the two cases for viscoelastic hemicylindrical soft fingertips were introduced and discussed. It is obtained that the control of the grasp forces (second case) when using viscoelastic contacts is most advantageous, because it promotes the stability of grasping through the enlargement of friction limit surface as time terminates. Finally, the viscoelastic limit surface results showed that the current model is more effective than previous model [13] at same conditions.

References

1. **T. Inoue and S. Hirai, "Mechanics and Control of Soft-fingered Manipulation," SPRINGER- VERLAG, London, 2008.**
2. **G. Carbone , "Grasping in Robotics". SPRINGER- VERLAG London, 2013.**
3. **V. L. Popove, "Contact Mechanics with Friction: Physical Principles and Applications," Publishing by Springer Berlin Heidelberg, 2010.**
4. **V. A. Yastrebov, "Numerical Methods in Contact Mechanics". First puplished by ISTE and John Wiley & Sons, Inc. 2013.**
5. **M. Erdmann, "On a representation of friction in configuration space". International Journal of Robotics Research, Vol. 13, No. 3, pp.240–271, 1994.**
6. **R. Howe, I. Kao, and M. Cutkosky, "Sliding of robot fingers under combined torsion and shear loading," Proceedings IEEE Int. Conf. on Robotics and Automation, pp. 103-105, 1988.**
7. **N. Xydas and I. Kao, "Modeling of contact mechanics and friction limit surface for soft fingers in robotics, with experimental results," Int. Jour. of Robotic Research, Vol.18, No.8, pp. 941–950, 1999.**
8. **Sadeq H. Bakhy, Shaker S. Hassan, Somer M. Nacy, K. Dermitzakis and, Alejandro H. Arieta, "Contact mechanics for soft robotic fingers: modeling and experimentation," Robotica / Volume 31 / Issue 04 / pp 599 609, July 2013.**
9. **Sadeq H. Bakhy, "Modeling of contact pressure distribution and friction limit surfaces for soft fingers in robotic grasping," Robotica, pp.1-11, Doi. 10.1017/S0263574713001215, © Cambridge University Press, 2013.**
10. **T. M. Junisbekov, V. N. Kestelman, and N. I. Malinin, "Stress relaxation in viscoelastic materials," Science Publishers Inc., 2002.**

11. **G. A. C. Graham, and J. R. Walton, "Crack and Contact Problems for Viscoelastic Bodies," SPRINGER- VERLAG London, 1995.**
12. **D. T. V. Pawluk and R. D. Howe, "Dynamic lumped element response of the human finger pad," ASME J. Biomech. Eng., vol. 121, no. 2, pp. 178–183, 1999.**
13. **P. Tiezzi and I. Kao, "Modeling of Viscoelastic Contacts and Evolution of Limit Surface for Robotic Contact Interface," IEEE TRANSACTIONS ON ROBOTICS, Vol. 23, NO. 2, APRIL 2007.**
14. **A. Touzaline, "Analysis of a viscoelastic frictionless contact problem with adhesion" REV. ROUMAINE MATH. PURES APPL., Vol. 55, No. 5, pp.411–430, 2010.**
15. **A. Freivalds, "Biomechanics of the Upper Limbs: Mechanics, Modeling and Musculoskeletal Injuries," Published by CRC Press, Second Edition, 2011.**
16. **P. Tiezzi and G. Vassura, "Experimental Analysis of Soft Fingertips with Internal Rigid Core", Proc. of Int. Conf. on Advanced Robotics ICAR 05, Washington, USA, July 18th-20th, 2005.**
17. **Sadeq H. Bakhy, "Mechanical Design and Analysis of a Robotic Human Hand for Prosthesis," Ph.D. University of Technology, Iraq, 2010.**
18. **H. Hertz, "On the contact of elastic solids," J. Reine Angew. Math. 92, 1881, pp. 156–171. Translated and reprinted in English in Hertz's Miscellaneous Papers, Macmillan & Co., London, 1896, Ch. 5. (Quoted by [19])**
19. **K. L. Johnson, "Contact Mechanics," Cambridge University Press, 1st edition, pp. 88-103. 1985.**
20. **W. N. Findley, J. S. Lai, and K. Onaran, "Creep and Relaxation of Nonlinear Viscoelastic Materials," Amsterdam, The Netherlands: North-Holland, 1976. (Quoted by [13]).**
21. **Y. C. Fung, "Biomechanics: Mechanical Properties of Living Tissues," New York: Springer-Verlag, 1993.**
22. **D. T. V. Pawluk and R. D. Howe, "Dynamic lumped element response of the human fingerpad," ASME J. Biomech. Eng., vol. 121, no. 2, pp. 178–183, 1999.**
23. **D. L. Jindrich, Y. Zhou, T. Becker, and J. T. Dennerlein, "Non-linear viscoelastic models predict fingertip pulp force-displacement characteristics during voluntary tapping," J. Biomech., vol. 36, no. 4, pp. 497–503, Apr. 2003.**
24. **L. Biagiotti, P. Tiezzi, C. Melchiorri, and G. Vassura, "Modelling and identification of soft pads for robotic hands," in Proc. IEEE Int. Conf. Intell. Robots Syst., Edmonton, AB, Canada, pp. 2786–2791, 2005.**
25. **P. Tiezzi, G. Vassura, L. Biagiotti, and C. Melchiorri, "Nonlinear modeling and experimental identification of hemispherical soft pads for robotic manipulators," in Proc. IDETC/CIE ASME Int. Des. Eng. Tech.l Conf./Comput. Inf. Eng. Conf., Long Beach, CA, Paper #DETC2005-85659, 2005.**

26. **F. Barbagli, A. Frisoli, K. Salisbury, and M. Bergamasco, "Simulating human fingers: A soft finger proxy model and algorithm," in Proc. IEEE Int. Symp. Haptic Interface, pp. 9–17, 2004.**
27. **H. Y. Han and S. Kawamura, "Analysis of stiffness of human fingertip and comparison with artificial fingers," in Proc. IEEE Int. Conf. Syst., Man, Cybern., 1999, pp. 800–805.**
28. **I. Kao and F. Yang, "Stiffness and contact mechanics of soft fingers in grasping and manipulation," IEEE Trans. Robot. Autom., vol. 20, no. 1, pp. 132–135, Feb. 2004.**
29. **P. Tiezzi and G. Vassura, "Experimental analysis of soft fingertips with internal rigid core," in Proc. IEEE Int. Conf. Adv. Robot., Seattle,WA, pp. 109–114, 2005.**
30. **W. N. Findley and J. S. Y. Lay, "A modified superposition principle applied to creep of non-linear viscoelastic material under abrupt changes in state of combined stress," Trans. Soc. Rheol., vol. 11, No. 3, pp. 361–380, 1967.**
31. **A. C. Pipkin and T. G. Rogers, "A non-linear integral representation for viscoelastic behaviour," J. Mech. Phys. Solids, vol. 16, pp. 59–74, 1968.**
32. **W. H. Yang, "The contact problem for viscoelastic bodies," Tras. ASME J. Appl. Mech., ser. E, vol. 33, pp. 395–401, 1966.**
33. **S. Attaway, " Matlab: A Practical Introduction to Programming and Problem Solving," Butterworth-Heinemann Publishing, 2013.**
34. **A. Deshpande, J. Ko, D. Fox, and Y. Matsuoka,"Control strategies for the index finger of a tendon-driven hand," he International Journal of Robotics Research, vol. 32, 1: pp. 115-128, January 2013.**
35. **D. Petković, J. Iqbal, S. Shamshirband, A. Gani, N. D. Pavlović, and L. Mat Kiah, "Kinetostatic Analysis of Passively Adaptive Robotic Finger with Distributed Compliance," Advances in Mechanical Engineering,Vol. 2014, 13 pages, 2014.**
36. **H. Cha, K. Koh, and B. Yi, " Stiffness modeling of a soft finger," International Journal of Control, Automation and Systems, Vol. 12, Issue 1, pp. 111-117, February 2014.**
37. **Cretu, A.M.; Payeur, P.; Petriu, E.M., "Soft object deformation monitoring and learning for model-based robotic hand manipulation," IEEE Trans. Syst. Man Cybern. Part B, Vol.42, pp.740–753, 2012.**
38. **C. Smith, Y. Karayiannidis, L. Nalpantidis, X. Gratal, P. Qi, D. Dimarogonas, and D. Kragic, "Dual Arm Manipulation - a Survey," Robotics and Autonomous Systems, Vol. 60, No. 10, pp. 1340-1353, 2012.**
39. **Z. Hurak and J. Zemanek, " Feedback linearization approach to distributed feedback manipulation ," American Control Conference (ACC), Montreal, QC , PP. 991 - 996, 27-29 June 2012.**
40. **Y. Karayiannidis, C. Smith, F. Vina, and D. Kragic, " Online Kinematics Estimation for Active Human-Robot Manipulation of Jointly Held Objects," 2013 IEEE/RSJ**

International Conference on Intelligent Robots and Systems, November 3-7, Tokyo, Japan, pp. 4872-4878, 2013.

41. B. Lei, S. Fei, and J. Zhai, "Robustly stable switching neural control of robotic manipulators using average dwell-time approach," Proceedings of the Institution of Mechanical Engineers, Part I: Journal of Systems and Control Engineering, March 2014; vol. 228, 3: pp. 154-166., first published on December 22, 2013.

Appendix

Equations Of Tangential Force And Moment In Constructing Limit Surface For Viscoelastic Contact Of Hemicylindrical Fingertips

The equations of tangential force and moment for viscoelastic fingers follow the same derivation depended on the scanning of instantaneous center of rotation (COR), initially utilized in [9]. The tangential force f_t over the entire contact area is the sum of the friction forces df_t, as illustrated in **Figure (11),** ruled by the Coulomb's law on the infinitesimal element dA.

$$\mathbf{f_t} = \begin{pmatrix} \mathbf{f_x} \\ \mathbf{f_y} \end{pmatrix} = -\int_{\mathbf{A}} \boldsymbol{\mu}\ \tilde{\boldsymbol{\upsilon}}(\mathbf{q})\, \mathbf{p}(\mathbf{q})\, \mathbf{dA} \qquad \mathbf{(A1)}$$

The vector $\tilde{\boldsymbol{\upsilon}}(\boldsymbol{q})$ in equation (A1) appears the unit vector along the direction of the velocity (opposite to the direction of df_t) with respect to the COR, as illustrated in figure (A1), μ is the coefficient of friction, and $p(q)$ is the pressure on the infinitesimal contact patch. Since the coordinate frame such that the COR is along the X axis, it can be concluded that $f_x = 0$ due to symmetry. So, the force vector in equation (A1) can be represented as a scalar $f_t = f_y$. The y -component of the unit vector can be used as [6]

$$\tilde{\upsilon}(\mathbf{q}) = \frac{\mathbf{1}}{\sqrt{(\mathbf{x}-\mathbf{d_c})^2 + \mathbf{y}^2}} \begin{bmatrix} -\mathbf{y} \\ (\mathbf{x}-\mathbf{d_c}) \end{bmatrix} \qquad \mathbf{(A2)}$$

where y, x,and d_c are the distances explained in figure (A1). Similarly, the moment about the normal to the contact area in the Z direction is

$$\mathbf{m_z} = \int_{\mathbf{A}} \boldsymbol{\mu}\, \|\mathbf{q} \times \tilde{\boldsymbol{\upsilon}}(\mathbf{q})\|\, \mathbf{p}(\mathbf{q})\ \ \mathbf{dA} \qquad \mathbf{(A3)}$$

Since m_z is along the Z direction, the scalar notation of m_z representing the magnitude will be utilized. The magnitude of the cross product in equation (A3) becomes

$$\|\mathbf{q} \times \tilde{\mathbf{v}}(\mathbf{q})\| = \frac{(\mathbf{x} - \mathbf{d_c})}{\sqrt{(\mathbf{x} - \mathbf{d_c})^2 + \mathbf{y}^2}} \qquad \mathbf{(A4)}$$

Note that equations (A1) and (A3) stay the same for viscoelastic contact, except that the terms f_t and m_z are now functions of time and depend on the nature of the load, because the pressure p is a function of time. By combining terms from equations (A1) to (A4), the following equations are derived:

$$\frac{\mathbf{f_t}}{\boldsymbol{\mu}\mathbf{N}} = \frac{\mathbf{C_k}}{2\boldsymbol{\pi}} \int_{-1}^{1}\int_{-1}^{1} \frac{(\tilde{\mathbf{x}} - \tilde{\mathbf{d}}_\mathbf{c})}{\sqrt{(\tilde{\mathbf{x}} - \tilde{\mathbf{d}}_\mathbf{c})^2 + (\mathbf{D} * \tilde{\mathbf{y}})^2}} \left(1 - \tilde{\mathbf{y}}^{\mathbf{k}}\right)^{\frac{1}{\mathbf{k}}} \mathbf{d}\tilde{\mathbf{y}}\, \mathbf{d}\tilde{\mathbf{x}} \qquad \mathbf{(A5)}$$

$$\frac{\mathbf{m_z}}{\mathbf{a}\boldsymbol{\mu}\mathbf{N}} = \frac{\mathbf{C_k}}{2\boldsymbol{\pi}} \int_{-1}^{1}\int_{-1}^{1} \frac{(\tilde{\mathbf{x}}^2 - \tilde{\mathbf{x}}\tilde{\mathbf{d}}_\mathbf{c} + (\mathbf{D} * \tilde{\mathbf{y}})^2)}{\sqrt{(\tilde{\mathbf{x}} - \tilde{\mathbf{d}}_\mathbf{c})^2 + (\mathbf{D} * \tilde{\mathbf{y}})^2}} \frac{\mathbf{1}}{\mathbf{D}} \left(1 - \tilde{\mathbf{y}}^{\mathbf{k}}\right)^{\frac{1}{\mathbf{k}}} \mathbf{d}\tilde{\mathbf{y}}\, \mathbf{d}\tilde{\mathbf{x}} \qquad \mathbf{(A6)}$$

Where $\tilde{x} = \frac{x}{b}$, $\tilde{d}_c = \frac{d_c}{b}$, $\tilde{y} = \frac{y}{a}$, $and \quad dA = dx\, dy = a\, b\, d\tilde{y}\, d\tilde{x}$

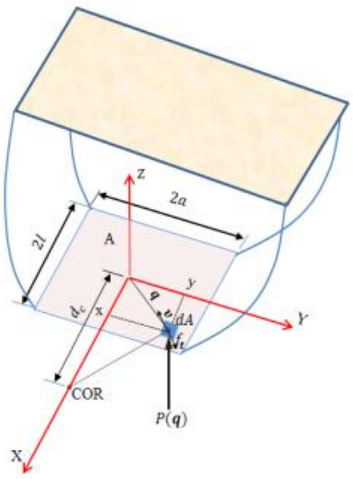

Fig . (A1): Contact and coordinates for COR and local infinitesimal area dA for numerical integration to construct the limit surface of hemicylindrical soft fingertips [9].